Technical Report

Development of Technology to Realize High-performance Integrated Parts Using Steel Sheets for Hot Stamping

Naoki KIMOTO*
Masahiro KUBO
Tasuku ZENIYA
Tohru OKADA
Shinichiro TABATA
Tohru YONEBAYASHI
Kenta IKEGAMI
Atsushi OHNO
Soshi FUJITA
Hiroshi YOSHIDA

Abstract

In automotive body structures, there is a demand for weight reduction, cost reduction, and GHG emission reduction while ensuring various performance characteristics. One of the means to meet these requirements is the component integration. Nippon Steel Corporation has developed hot stamping steel sheets with various strength characteristics and deformation capabilities, and by introducing the utilization technologies such as structural design and forming methods that leverage these properties, this study provide an overview of the comprehensive efforts to realize high-performance integrated components.

1. Introduction

1.1 Background: demands on automobiles

To achieve carbon neutrality by 2050, reducing life cycle greenhouse gas (LC-GHG) emissions is essential. In the automotive industries, Battery Electric Vehicles (BEVs) have become rapidly widespread in recent years.[1)] However, the batteries in BEVs weigh several hundred kilograms, significantly increasing the vehicle's total weight. Consequently, the vehicle body structure is needed to meet higher collision performance standards than ever before. Furthermore, the high manufacturing cost of batteries contributes to the overall increase in vehicle prices. Therefore, automotive body structures is needed to improve both collision performance and reduce costs. Furthermore, due to the declining working population caused by a low birth rate and aging society, along with changes in career aspirations, labor-saving technologies are needed in the automotive industries. To meet these demands, Tesla developed Gigacast—an innovative die-casting technology that forms large aluminum components as a single piece. Tesla has integrated approximately 70 components of the rear underbody into a single giga cast part with this technology, improving production efficiency.[2)] Giga-cast parts have issues such as requiring new large-scale equipment during production, reduced repairability in minor collisions, and being unsuitable for the production of many vehicle models.[3)] In response to this, automobile manufacturers are reconsidering the optimization of their vehicle body manufacturing processes.

As described above, the automotive industry is undergoing major transformations, including stricter environmental regulations, the proliferation of electric vehicles, changes in body structures, and innovations in manufacturing technology. To respond to these changes, Nippon Steel Corporation has developed the next-generation automotive concept "NSafe™-AutoConcept". This report and the next report (Table of Contents No. 7) introduce the concept and various key technologies developed to contribute to reducing total cost, GHG emissions, and weight, targeting integrated components as shown in **Fig. 1**. This report introduces technologies utilizing hot stamping steel sheets, while the next report will introduce technologies utilizing cold-formed high-tensile steel.

1.2 Overview of integrated technology

Automotive body structures require different strength characteristics and deformation capabilities for each part. As shown in **Fig. 2**, Nippon Steel has developed a total solution with a various material lineup and the structural, manufacturing, and evaluation technologies to utilize them. This enables the development of technologies to realize high-performance integrated components that accurately meet various requirements across scales from small/medium to large.

As shown in the upper left of Fig. 2, we have developed latest

* Researcher, Integrated Steel-Solution Research Lab.-I, Steel Research Laboratories
20-1 Shintomi, Futtsu City, Chiba Pref. 293-8511

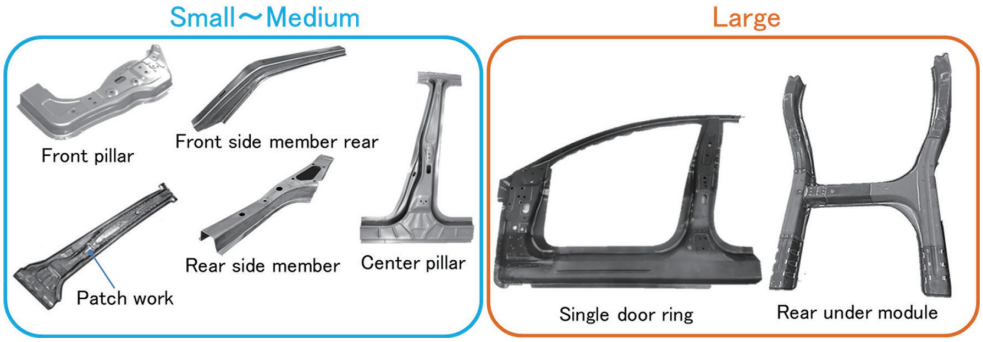

Fig. 1 Examples of the integrated components

Fig. 2 Total solution for high-performance integrated parts

high-strength steel sheets like 2.0 GPa-grade hot stamping steel (HS) and high-deformation, high-energy-absorption materials (e.g., 0.5 GPa, 1.0 GPa, and 1.3 GPa-grade HS). By utilizing tailored welded blank (TWB) technology, it is possible to use these various materials in the most suitable locations, enabling significant weight reduction, greenhouse gas emissions reduction, and cost reductions.

Examples of small- to medium-scale parts integration include patchwork technology[4] that press-forms two stacked parts at once, and a method of reducing reinforcement members by increasing the strength of the main frame (Fig. 1, left). For large-scale component integration to shorten assembly lines, hot stamping technology is an effective method. Examples include door rings, which have been in practical use since the 2010s, and rear under modules, proposed around 2020 (Fig. 1, right).

2. Development Concept

2.1 Overview of the structure

Nippon Steel has developed a concept for large-scale integrated components utilizing hot stamping steel sheets, with an example shown in **Fig. 3**. Figure 3 shows the rear under module, composed of (a) the upper side and (b) the lower side. The material used is hot stamping aluminum-coated steel sheet. 2.0 GPa-HS is applied in front section of the side member to suppress deformation, 1.0 GPa-HS is applied in rear section of the side member to energy absorption through axial compression, and 1.5 GPa-HS is applied in the other section. These materials are joined by TWB. Depending on the required characteristics, TWB is implemented either by spot welding or by butt laser welding. For laser-welded TWB, new welding techniques enable enhance the welding strength. For spot-welded TWB, innovations in processes and press forming methods enable to achieve a structure equivalent to conventional split structures even in integrated parts. Finally, the upper wheel house is integrated with the lower side members and floor. To achieve this structure, a dual-axis hot stamping process utilizing a cam mechanism is developed. Details of these key technologies are presented in Chapter 3.

2.2 Performance of the development concept

Figure 4 shows the estimated results for weight and GHG emissions over the life cycle for the rear under module. Integrated structure using hot-stamped steel sheets, the conventional steel and aluminum mixed structure, and the aluminum die-cast structure, all with equivalent rear impact performance, are compared. The GHG emission calculation follows the method described in the separate report (Table of Contents No. 5) on Life Cycle Assessment (LCA).

As shown in Fig. 4 and **Table 1**, the developed integrated structure shows superior results in GHG emissions and weight and cost compared to the conventional steel and aluminum mixed structure and the aluminum die-cast structure. Notably, the integrated structure shows significantly superior results compared to the aluminum die-cast structure. Aluminum die-cast parts require control of the structure and sheet thickness to design various strength levels, since the strength of aluminum is constant. For this reason, weight reduc-

tion with aluminum die-casting is difficult. On the other hand, steel sheet with TWB enable weight reduction by allocating strength and sheet thickness in suitable locations.

Therefore, using the integrated structure with hot stamping steel contributes to reducing the cost and weight of automotive bodies, GHG emissions over the life cycle.

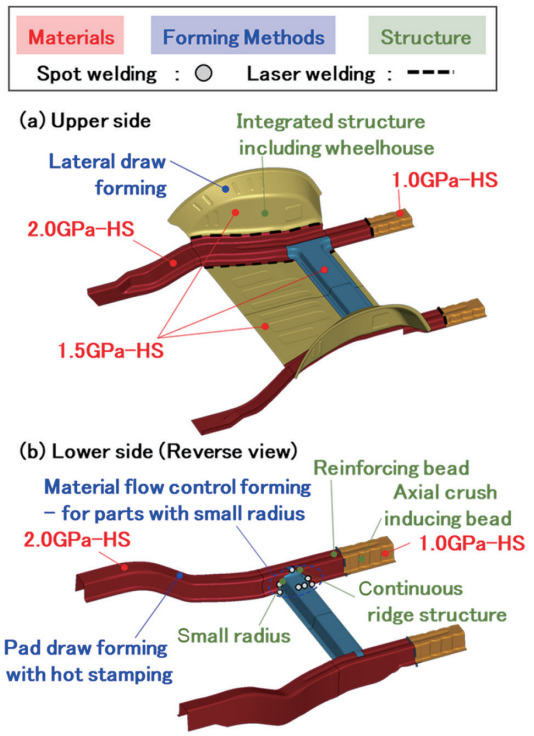

Fig. 3 Integrated rear under module concept with large-scale hot stamping

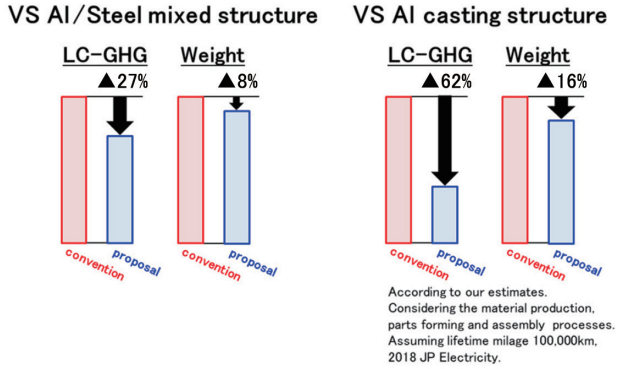

Fig. 4 LC-GHG, weight of integrated steel structure compared to Al/Steel mixed and Al casting structure

Table 1 Comparison of cost, LC-GHG, weight

Type	Cost	LC-GHG	Weight
Integrated hot stamping structure	Good	Good	Good
Al/steel mixed structure	Poor	Poor	Poor
Al casting structure	Very poor	Very poor	Poor

3. Key Technologies

3.1 Utilization technology for 2.0 GPa-grade hot stamping steel

As shown in Fig. 2, 2.0 GPa-HS has been commercialized as a latest high-strength steel sheet.[5] Applying 2.0 GPa-HS to body frame members is expected to enable part reduction and weight reduction by eliminating reinforcement members conventionally placed to ensure member strength. **Figure 5** shows an example of part count reduction and weight reduction using 2.0 GPa-HS in a center pillar.[6] Compared to using 980 MPa-grade steel sheet, applying 2.0 GPa-HS is estimated to enable a 29% weight reduction and eliminating reinforcement members.

Hot-stamped components primarily achieve strength through the utilization of a martensitic microstructure. While increasing carbon content can enhance the strength of this microstructure, this strength increase is accompanied by a decrease in toughness. Consequently, it is anticipated that material fracture during collision deformation may prevent the achievement of sufficient performance. Furthermore, hydrogen embrittlement cracking, which occurs when material strength, diffusible hydrogen content, and tensile residual stress meet certain conditions, tends to become more susceptible with increased strength. To address these challenges, countermeasures are being developed on both the material and application technology. In terms of materials development, toughness and hydrogen embrittlement resistance have been improved through composition design, so application is expected in underbody areas, such as the rear underbody module shown in Fig. 3.

In terms of applied technology development, new technologies have been developed to suppress fracture during collision deformation. For example, adding bead to wall surfaces of the frame is expected to suppress fracture by dispersing strain during bending deformation.[7] **Figure 6** shows the results of a partial structure side impact test simulating a side pole collision with a front pillar using 2.0 GPa-HS. These results shows that the bead suppresses the fracture of the material.

During the collision deformation of high-tensile steel sheets, fractures from spot welds or the heat-affected zone (HAZ) are also anticipated. Details of countermeasures are described in another report (Table of Contents No. 12). Effective measures against spot weld fractures include improving joint strength through optimization of welding conditions[8] and reducing stress through structural optimization[9]. Furthermore, countermeasures against fracture from the HAZ include controlling hardness distribution around the HAZ by tempering and reducing tensile loads through optimization of the structure[10–12].

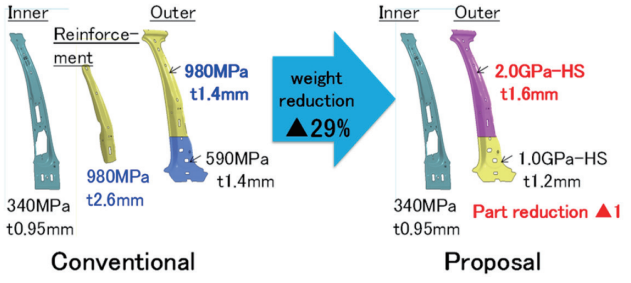

Fig. 5 Example of part reduction and weight reduction using 2.0 GPa hot stamping steel

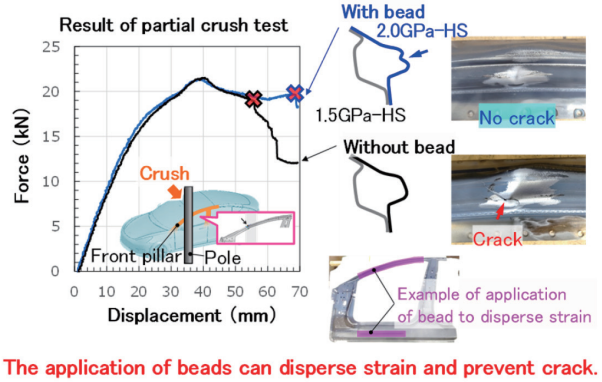

Fig. 6 Cross sectional design that disperses strain during collision deformation

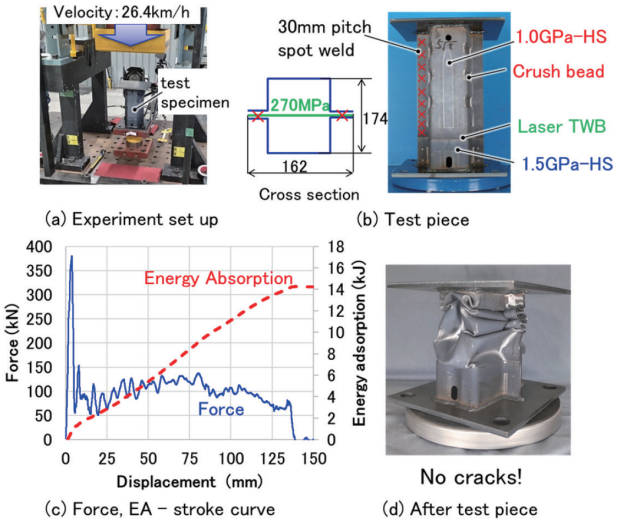

Fig. 7 Effect on 1.0 GPa hot stamping steel in axial crush test

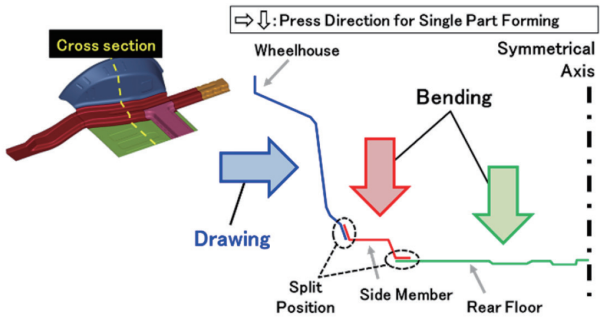

Fig. 8 Cross-sectional diagram of upper side of rear under module

3.2 Utilization technology for hot-stamped steel sheets for energy-absorbing components

In the event of a frontal collision (or rear collision), crash boxes and front side members (rear side members) may be designed to absorb collision energy by undergoing significant deformation, thereby preventing damage to the cabin. One example of deformation in crash boxes and front side members (rear side members) is axial compression, where the material folds like an accordion while deforming. For components undergoing axial compression, it is essential to prevent discontinuities in deformation progression caused by fracture. Until the 2010s, the primary application is 590 MPa-grade steel sheets. Therefore, in order to reduce the weight of components subjected to axial compression, materials with a balanced combination of strength and deformability (particularly bendability) have been developed. Examples include 980EA steel sheets for cold-formed high-strength steel and 1.0 GPa-class materials for hot-stamped steel sheets.

Figure 7 shows the results of a dynamic axial compression test using 1.0 GPa-HS applied to a hat-shaped member simulating the rear side member. In order to achieve high energy absorption, it is important to ensure buckling stability. Therefore, beads with adjusted shapes (width and depth) are arranged on the members to control buckling. The crush test utilized the crush test apparatus at Nippon Steel's Hasaki Research Center. Test results showed axial compression along the buckling beads without fracture.

3.3 New method for forming complex structures using a cam mechanism: biaxial hot stamping method

In component integration using the rear under module, H-shaped frames integrating side members and cross members[13] have been reported previously. Furthermore, integrating the wheelhouse into the rear under module's integrated structure is expected to further reduce the number of parts and enhance side impact resistance. **Figure 8** shows a cross-section of the upper side of the rear under module. This section consists of components such as the wheel house, side member, and rear floor. The arrows in the figure indicate the press direction and forming method when each component is formed individually. The side member and rear floor are often press-formed by bending deformation in a posture nearly identical to the vehicle assembly posture. Conversely, the wheel house is frequently deep-drawn in a posture rotated approximately 90° from the vehicle assembly posture. Therefore, the forming process becomes more difficult because parts that have different forming methods and require pressing directions approximately 90° apart must be formed simultaneously.

A new method has been developed: the dual-axial hot stamping method.[13] The mold structure is shown in **Fig. 9**. The die positioned beneath the blank is divided into three sections: a cam 1 forming the flange of the wheel house, a cam 2 forming the main part of wheel house, and a cushion forming the rear floor and side member sections. The die structure is designed so that two cams are driven at the intended timing by a single cam driver. Specifically, after holding the blank with the upper cam 1 and the die, and the cushion and die, the lower cam 2 is driven to form the wheel house.

The effectiveness of this development method concept is verified using forming analysis with AutoForm R10. The test specimen is configured with the material properties of hot-stamped steel sheet (22MnB steel), and the analysis accounted for material temperature changes and phase transformations during hot stamping. The steel sheet is heated to 920°C, and forming begins 18 seconds after it is taken out of the heating furnace.

Figure 10 shows the forming analysis results by developed method. The maximum thickness reduction rate is approximately 20%, indicating the potential to achieve large-scale integral forming while suppressing fracture and wrinkles.

Figure 11 shows images of the prototype parts. The forming conditions are the same as those used in the forming analysis. The actually formed parts are also confirmed to be feasible, with no noticeable wrinkles or fracture.

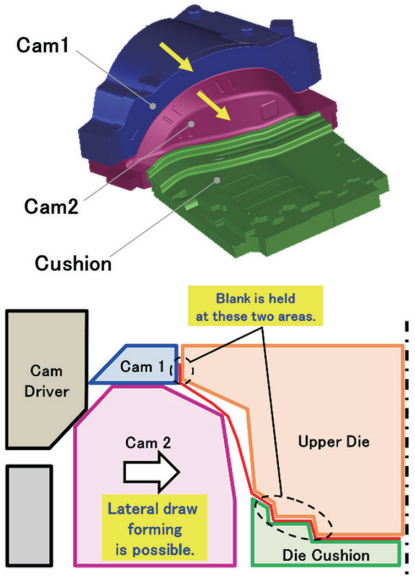

Fig. 9 Cross-sectional diagram of die structure in developed method

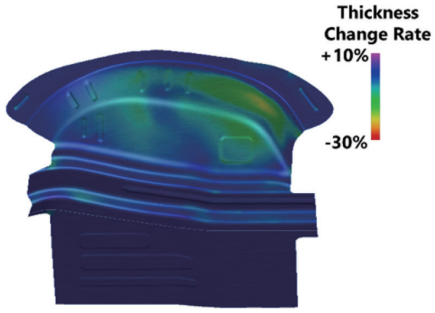

Fig. 10 Forming analysis results by developed method

Fig. 11 Prototype by developed method

3.4 New method for improving formability of integrated parts by controlling material flow

In general, it is difficult to form parts where multiple frames intersect. Examples include the joint between the lower front pillar (or center pillar) of the door ring and the side sill, and the joint between the rear side member and cross member of the rear under module. At these junctions, fracture and wrinkles are likely to occur due to sudden changes in the cross-sectional line length (**Fig. 12**). This suggests that the conventional structure cannot simply be replaced with an integrated structure, and a significant redesign of the surrounding component layout will be required.

Therefore, a new forming method is developed to enhance the design freedom of the corner radius R at component joints in integrated parts.[7, 14–16] A schematic is shown in **Fig. 13**. When TWB is placed at the junctions between parts, by partially joining the junctions with TWB before forming and forming the remaining parts afterward, the material flow during forming is facilitated. This suppresses fracture and wrinkling at corners and joints. Hereafter, we introduce the details of this technology using TWB as spot-welded TWB.

We developed two distinct methods adaptable to the desired structure: the TWB Material Flow Control Overlap Method[7, 14, 15] (Fig. 13(a)) and the Integrated Small Corner R Method[16] (Fig. 13(b)). The TWB Material Flow Control Overlap Method allows for a wide overlap between the components forming the joint. By limiting the pre-formed welding areas to regions with minimal material flow, the flow of the material can be promoted, thereby improving formability. In areas where material flow is significant, spot

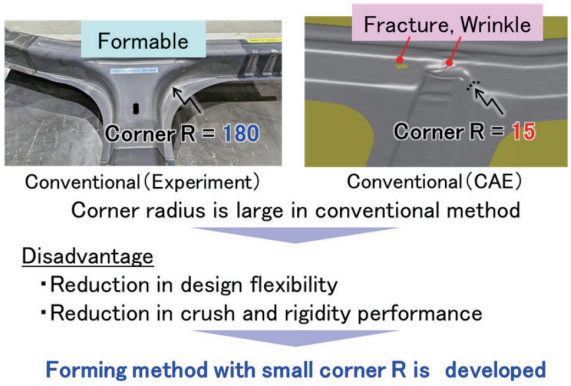

Fig. 12 Subject to conventional forming method

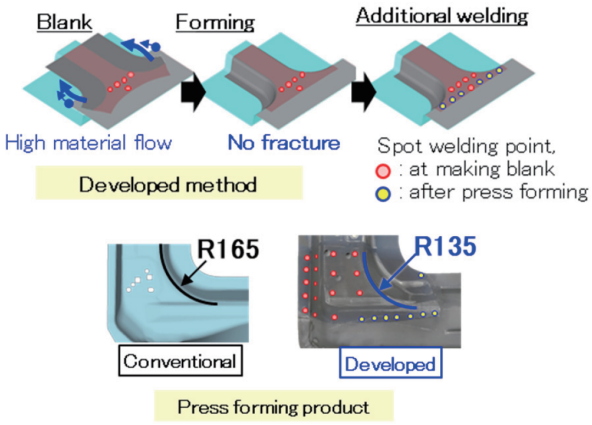

(a) TWB material flow control overlap method

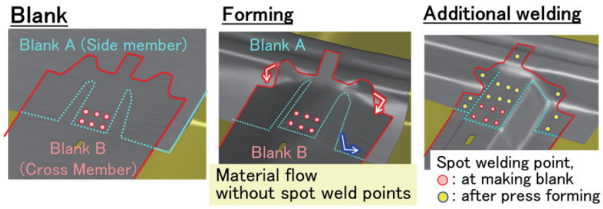

(b) Integrated small corner R developed method

Fig. 13 Overview of spot TWB utilization forming method

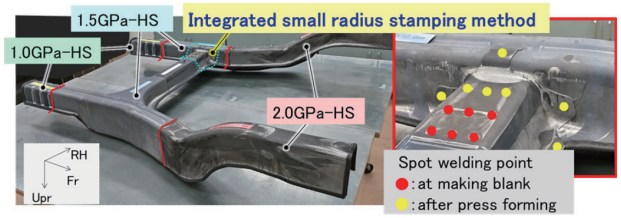

Fig. 14 Development methods applied to rear under module

welding is performed after forming. Examples of application include the joints between the front pillar and the side sill, or between the center pillar and the side sill. The overlap can be adjusted to ensure rigidity at the door mounting positions, or it can be used to control collision deformation modes.

The integrated small corner R method shares the basic concept with the TWB Material Flow Control Overlap Method. By adjusting the blank shape to promote material flow, it becomes possible to form parts with smaller corner R. Therefore, this method is applicable in locations with strict layout constraints. Examples include the junctions between the rear side member and cross member, and the junctions between the floor tunnel and floor cross member. By selecting the appropriate forming method according to the structure, it contributes to the realization of high-performance integrated components.

Figure 14 shows an example of applying the integrated small corner R forming method to the lower component of the rear under module. 1.5 GPa-HS is used on the side member and on the cross member. The red dots in the figure indicate spot weld points before forming and the yellow dots indicate spot weld points after forming. Forming is achieved without fracture or wrinkling.

3.5 Laser welding solution technology for TWB sections

The previous section discussed TWB using spot welding. This section introduces TWB technology using butt laser welding. Compared to conventional structures, butt laser welding can reduce the overlap area, enabling weight reduction.

3.5.1 Challenges in TWB sections using butt laser welding for hot stamping aluminum-coated steel sheets

It is known that laser welding of aluminum-coated steel sheets results in significant Al contamination in the weld metal.[17] It has also been reported that in butt welds like TWB achieved by laser welding, Al migrates from the molten boundary on the steel sheet surface, creating localized Al enrichment zones within the weld metal.[18] As the Al content increases, the Ac3 point rises. Consequently, in TWB formed by butt laser welding of aluminum-coated steel sheets, the weld metal may not undergo sufficient austenitic transformation at the hot stamping heating temperature, resulting in insufficient quenching. This leads to lower hardness compared to the base material. As a result, joint strength may decrease, potentially causing fracture in the weld metal zone under load. In other words, controlling the Al concentration in the weld metal to an appropriate level is crucial. However, as mentioned above, the Al concentration in the weld metal is not uniform, making it unavoidable that localized softened areas, which could become fracture initiation points, are incorporated. Therefore, it is necessary to appropriately remove Al near the molten boundary, which is the source of Al inclusion, prior to welding.

3.5.2 Overview of TWB technology using butt laser welding and joint performance

Figure 15 shows a schematic diagram of the TWB manufacturing process using butt laser welding with Nippon Steel's hot stamping aluminum-coated steel sheets. First, an end mill is used to mechanically remove the aluminum coating from the steel sheet surface near the butt joint end face of each steel sheet. To achieve this, micron-level precision cutting technology is developed. Next, the cut end faces of each steel sheet are butted together and welded. In the TWB of hot stamping steel sheets, the hardness of the weld metal, HAZ, and base material becomes nearly equivalent during the heating process. To avoid strain concentration in the thinned areas during forming, filler-added laser welding is used to ensure the weld metal thickness is greater than the thickness of the plating-removed area on the thinner sheet side.

As an example, butt welded joints are fabricated using 1.2 mm thick aluminum-coated 1.3 GPa-HS and 1.6 mm thick aluminum-coated 2.0 GPa-HS, employing both the developed technology and a comparative technology. The results of investigating the joint properties are described below. The comparative technology involved laser welding without filler metal and without removing the aluminum cladding. **Figure 16** shows the Al mapping results from EPMA analysis of the weld cross-section. In the comparative technology, a large amount of Al is mixed into the weld metal relative to the base metal, and localized Al enrichment is observed near the fusion boundary. In contrast, the developed technology suppressed Al mixing into the weld metal, and no localized Al enrichment is observed. **Figure 17** shows the Vickers hardness distribution of the weld. Additionally, **Fig. 18** shows the post-tensile test appearance of the joint. With the comparison technology, the weld metal hardness is generally lower than the base metal hardness on the low-strength steel sheet side. Locally, areas within the weld metal showing hardness reductions of approximately HV100 are observed. In contrast, with the developed technology, the weld metal hardness is higher than the base metal hardness on the low-strength steel sheet side and generally increased monotonically from the low-strength steel sheet side to the high-strength steel sheet side. Consequently, in the tensile test of the joint, fracture occurred in the weld metal with the comparison technology, whereas fracture occurred in the base metal with the developed technology, confirming the high reliability of the joint.

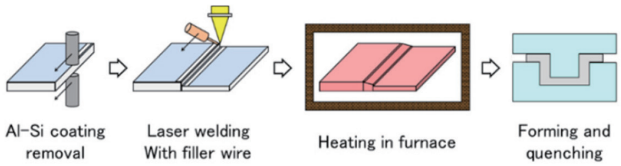

Fig. 15 TWB process of Al coated hot stamping steel

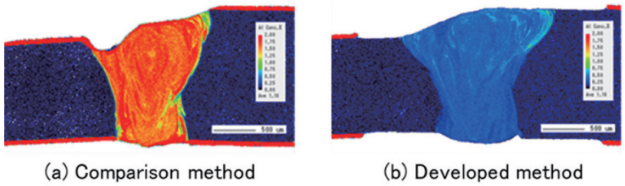

Fig. 16 EPMA analysis of Al

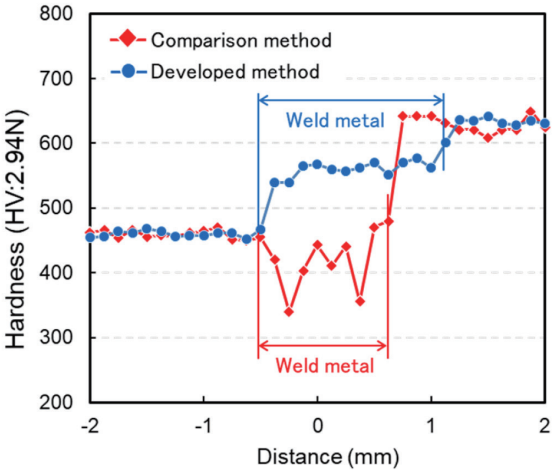

Fig. 17 Hardness distribution of hot stamped laser welds

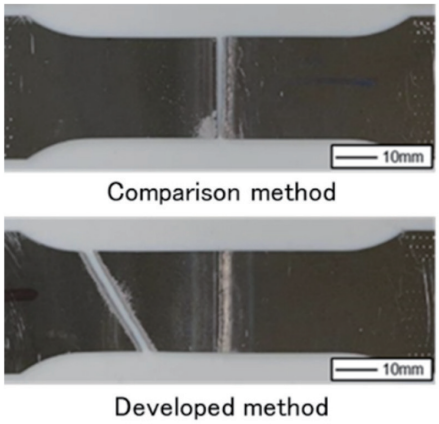

Fig. 18 Test specimen after tensile test

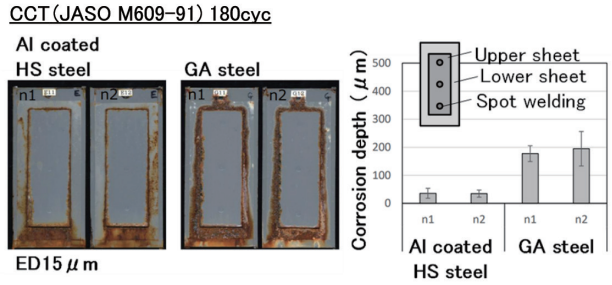

Fig. 19 Corrosion resistance of overlapping parts

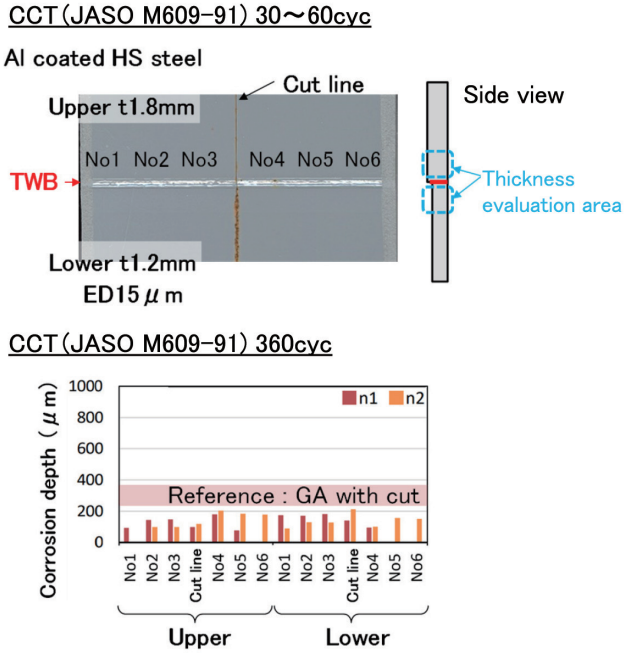

Fig. 20 Corrosion resistance of around the TWB area

3.6 Corrosion resistance of the joint

The corrosion resistance of hot stamping aluminum-coated steel sheets (coating weight 160 g/m^2 on both sides) has been reported to be equivalent to that of conventional rust-proof steel sheets, such as hot-dip galvannealed steel sheets (GA) or galvanized steel sheets (GI).[19–22] For the integrated components, key differences compared to conventional parts include the presence of overlapped sections formed by patchwork methods or TWB by spot welding, and TWB by butt laser welding. Examples of corrosion resistance evaluation are presented below.

Figure 19 shows an example of corrosion resistance evaluation for a test specimen where two steel sheets are overlapped via spot welding and then E-coating (film thickness 15 μm). Corrosion occurs near the overlap boundary of the hot stamping aluminum-coated steel sheets. However, after corrosion progressed to 180 cycles, corrosion resistance (corrosion depth) is equivalent to or better than that of GA.

Figure 20 shows an example of corrosion resistance evaluation for a test specimen with E-coating (film thickness 15 μm) applied to the TWB section created by butt laser welding. Corrosion occurs at the butt welded TWB section with a cut, but no noticeable rust is observed up to 30–60 cycles. When corrosion progressed to 360 cycles, equivalent or superior corrosion resistance (corrosion depth) is achieved compared to GA with a cut (approximately 300 μm sheet thickness reduction).

4. Performance Evaluation Using Prototype Equipment

4.1 Test specimen

Figure 21 shows a view of the test specimen from the underside of the vehicle. 2.0 GPa-HS is applied in front section of the side member to suppress deformation, 1.0 GPa-HS is applied in rear section of the side member to energy absorption through axial compression, and 1.5 GPa-HS is applied in the other section. TWB joints using butt laser welding are placed at the material joints of the rear side members. TWB joints using spot welding are placed at the joints between the rear side members and cross members. The upper and lower sections are joined by spot welding. Additionally, end plates are arc-welded to the front and rear ends of the test specimen.

4.2 Test method

The crush test utilized the large scale crush test apparatus at Nippon Steel's Hasaki Research Center.[23] **Figure 22** shows the appearance of the large scale crush test apparatus. The test specimen is fixed on the fixture with the vehicle rear facing upward. Evaluation

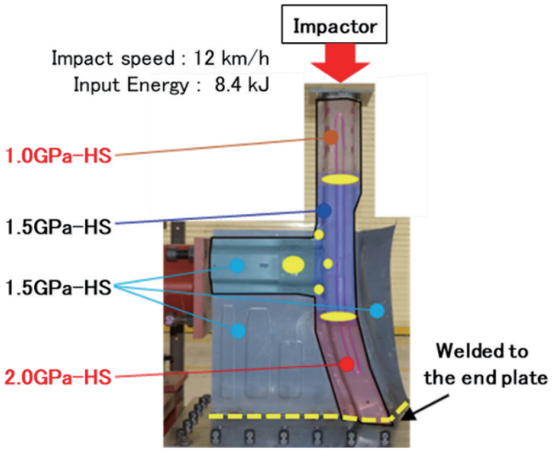

Fig. 21 Integrated rear module crush test specimen

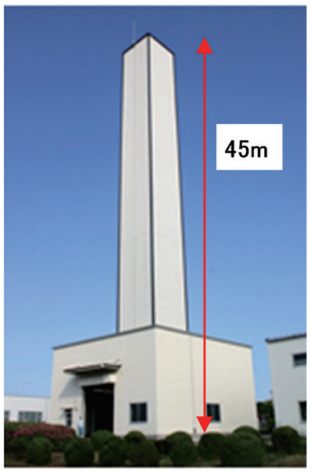

Fig. 22 Large-scale crush test apparatus

is performed by dropping a rigid impactor so that its flat surface collided with the test specimen. The collision speed is set at 12 km/h. This is calculated based on the energy absorption of 8.4 kJ estimated beforehand through numerical analysis. Since the test specimen comprised only the right half of the vehicle, a support fixture is installed at the cross-member end to prevent lateral tilting. This evaluation aimed to confirm whether the vehicle front end withstands buckling and whether the rear energy-absorbing section undergoes axial crushing deformation without base material fracture to absorb energy.

4.3 Test results

Figure 23 shows the force-displacement diagram. After the load reached its maximum value around a displacement of 10 mm, it fluctuated slightly around approximately 100 kN. Figure 23 shows the test specimen after crush test. The validity of the design concept is confirmed: the front section using 2.0 GPa-HS material withstood the collision load, while the rear section using 1.0 GPa-HS material absorbed energy through axial compression.

It is generally a concern that the intersection between the rear side member and the cross member may become a weak point against rear impacts because the vertical wall eliminated. Therefore, in this integrated rear under module structure, the integrated small

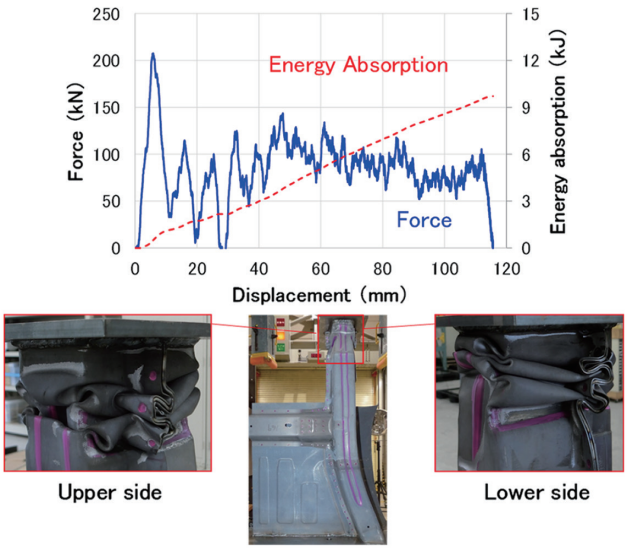

Fig. 23 Crush test results for integrated rear module

corner R method is applied to preserve ridge line of the rear side member. The crush test results confirmed that, as intended, the structure withstood the load without buckling even in the area where the vertical wall is eliminated. Furthermore, no fractures are observed in the floor panel or wheelhouse, which utilized 1.5 GPa-HS.

Based on the above, it is confirmed that by combining appropriate material selection, structural design that leverages these materials, and construction methods that realize them, it is possible to achieve high-performance integrated components in an integrated structure.

5. Conclusion and Future Prospects

A total solution technology has been developed that integrates materials, structural design, manufacturing processes, and evaluation methodologies, thereby enabling the realization of high-performance integrated components using hot-stamped steel sheets. This approach allows not only for vehicle weight reduction and enhanced crashworthiness, but also for significant reductions in manufacturing costs and GHG emissions. By comprehensively applying these technologies, precise responses to diverse requirements can be achieved, facilitating the integration of components from small and medium to large scales. Key technologies include the utilization of 2.0 GPa-class and 1.0 GPa-class hot-stamped steel sheets, advanced forming processes for complex integrated component geometries, and joining technologies for TWB sections.

Moving forward, further development of total solution technologies is planned. This includes the creation of materials with superior energy absorption capabilities at strengths of 980 MPa and above, along with their associated solution technologies; the application of the integrated forming technologies described herein to additional modules, beginning with battery boxes; and the advancement of construction methods to realize closed cross-sections through integrated forming. Through these efforts, a high level of achievement in automotive weight reduction, manufacturing cost reduction, and lifecycle GHG emission reduction is expected to be realized.

References

1) Kubo, M. et al.: Proceedings of the 2022 JSAE Annual Congress (Spring), Document No. 20225281 (2022)

2) Visnic, B.: Tesla casts a new strategy for lightweight structures: Automot. Eng. SAE Int. (2020), p. 12–13
3) Volk, W.: Gigacasting ist geeignet, den Karosseriebau neu zu denken: Automobilproduktion
4) https://www.nipponsteel.com/news/20220622_100.html
5) https://www.nipponsteel.com/news/20220830_200.html
6) https://www.nipponsteel.com/news/20220328_100.html
7) Kimoto, N. et al.: Proceedings of the 2024 JSAE Annual Congress (Spring), Document No. 20245115 (2024)
8) Furusako, S. et al.: Nippon Seitetsu Giho. (412), 11 (2019)
9) Koga, A. et al.: Transactions of the Society of Automotive Engineers of Japan. 49 (6), 1255 (2018)
10) Hirose, S. et al.: Transactions of the Society of Automotive Engineers of Japan. 50 (2), 570–574 (2019)
11) Hirose, S. et al.: Transactions of the Society of Automotive Engineers of Japan. 50 (6), 1679–1684 (2019)
12) Hirose, S. et al.: Transactions of the Society of Automotive Engineers of Japan. 51 (1), 215–220 (2020)
13) Ikegami, K. et al.: Proceedings of the 75th Japanese Joint Conference for the Technology of Plasticity, 223 (2024)
14) Kubo, K. et al.: 2024 Japanese Spring Conference for the Technology of Plasticity, 301 (2024)
15) Kimoto, N. et al.: Press Technology. November 2024 issue
16) Yonebayashi, T. et al.: Proceedings of the 75th Japanese Joint Conference for the Technology of Plasticity, 224 (2024)
17) Saita, K. et al.: Quarterly Journal of the Japan Welding Society. 27 (2), 145–153 (2009)
18) Shehryar Khan, M. et al.: Science and Technology of Welding and Joining. 25 (6), 447–467 (2020)
19) Suehiro, M. et al.: Shinnittetsu Giho. (378), 15 (2003)
20) Maki, J. et al.: CHS2 2011 p. 499 (2011)
21) Dosdat, L. et al.: Steel Research. 82 (6), 726 (2011)
22) Kusumi, K. et al.: Shinnittetsu Giho. (393), 8 (2012)
23) https://www.nipponsteel.com/tech/nssmc_tech/car/car_02/03.html

Naoki KIMOTO
Researcher
Integrated Steel-Solution Research Lab.-I
Steel Research Laboratories
20-1 Shintomi, Futtsu City, Chiba Pref. 293-8511

Atsushi OHNO
Senior Researcher
Integrated Steel-Solution Research Lab.-I
Steel Research Laboratories

Tohru YONEBAYASHI
Senior Researcher
Integrated Steel-Solution Research Lab.-I
Steel Research Laboratories

Tohru OKADA
Ph.D., Senior Manager, Head of Section
Welding & Joining Research Lab.
Steel Research Laboratories

Masahiro KUBO
Ph.D., Senior Researcher
Integrated Steel-Solution Research Lab.-I
Steel Research Laboratories

Soshi FUJITA
Senior Researcher, Head of Section
Kyushu R & D Lab.

Kenta IKEGAMI
Quality Management Div.
Nagoya Works

Shinichiro TABATA
Senior Researcher
Kyushu R & D Lab.

Tasuku ZENIYA
Senior Researcher
Integrated Steel-Solution Research Lab.-I
Steel Research Laboratories

Hiroshi YOSHIDA
Ph.D., General Manager, Head of Div.
Welding & Joining Research Lab.
Steel Research Laboratories